BIOLOGY OF ZIKA VIRUS INFECTION IN HUMAN SKIN CELLS

Running Title: Cellular tropism and entry receptors of Zika virus

Rodolphe Hamel[1], Ophélie Dejarnac[2$], Sineewanlaya Wichit[1$], Peeraya Ekchariyawat[1], Aymeric Neyret[3], Luplertlop Natthanej[4], Manuel Perera-Lecoin[1], Pornapat Surasombatpattana,[5] Loïc Talignani[1], Frédéric Thomas[1], Van-Mai Cao-Lormeau[6], Valérie Choumet[7], Laurence Briant[3], Philippe Desprès[8], Ali Amara[2], Hans Yssel[9] and Dorothée Missé[1#]

[1]Laboratoire MIVEGEC, UMR 224 IRD/CNRS/UM1, Montpellier, France

[2]Inserm, U944, Laboratoire de Pathologie et Virologie Moléculaire, Paris, France

[3] Centre d'étude d'agents Pathogènes et Biotechnologies pour la Santé, CNRS-UMR 5236/UM1/UM2, Montpellier, France

[4]Department of Microbiology and Immunology, Faculty of Tropical Medicine, Mahidol University, Bangkok, Thailand

[5]Pathology Department, Prince of Songkla University, Songkla, Thailand

[6]Institut Louis Malardé, Papeete, Tahiti, French Polynesia

[7]Unit Environment and Infectious Risks, Institut Pasteur, Paris, France

[8]Département infections et Epidémiologie, Institut Pasteur, 75724 Paris et UMR PIMIT (I2T team), Université de La Réunion, Inserm U1187, CNRS 9192, IRD 249, GIP-CYROI, 97491 Saint Clotilde, La Réunion, France.

[9] Centre d'Immunologie et des Maladies Infectieuses, Inserm, U1135, Sorbonne Universités, UPMC, APHP Hôpital Pitié-Salpêtrière, Paris, France

Word count for the abstract: 249

Word count for the text: 7039

Abbreviations: ZIKV**,** Zika virus; DENV, Dengue Virus; WNV, West Nile virus; PRRs, pattern recognition receptors; TLR, Toll-like receptor; RIG-I, retinoic acid-inducible gene 1; MDA-5, melanoma differentiation-associated gene 5; ISG, interferon-stimulated gene; DC-SIGN, dendritic cell-specific intracellular adhesion molecule 3-grabbing non-integrin; Ae., *Aedes*; CLEC5, C-type lectin domain family 5; IU, international Unit; LC3, cytosolic microtubule-associated light chain 3; OAS, oligoadenylate synthetase.

Keywords: Zika, arbovirus, Dengue, skin, fibroblast, keratinocyte, dendritic cells, AXL, Phosphatidylserine receptor, antiviral response, autophagy, flavivirus.

$ contributed equally to this work

Corresponding author: Address correspondence to Dorothée Missé, Email: dorothee.misse@ird.fr

ABSTRACT

Zika virus (ZIKV) is an emerging arbovirus of the *Flaviviridae* family that includes Dengue, West Nile, Yellow Fever and Japanese encephalitis viruses, causing a mosquito-borne disease transmitted by the *Aedes* genus, with recent outbreaks in the South Pacific. Here, we determine the importance of the human skin in the entry of ZIKV and its contribution to the induction of anti-viral immune responses. We show that human dermal fibroblasts, epidermal keratinocytes and immature dendritic cells are permissive to the most recent ZIKV isolate, responsible for the epidemic in French Polynesia. Several entry and/or adhesion factors, among which DC-SIGN, AXL, TYRO3, and to a lesser extent, TIM-1, permitted ZIKV entry with a major role for the TAM receptor AXL. ZIKV permissiveness of human skin fibroblasts was confirmed by the use of a neutralizing Ab and specific RNA silencing. ZIKV induced the transcription of TLR-3, RIG-I and MDA5, as well as several interferon-stimulated genes, including OAS2, ISG15 and MX1, characterized by a strongly enhanced interferon-β gene expression. ZIKV was found to be sensitive to the antiviral effect of both type I and type II interferons. Finally, infection of skin fibroblasts resulted in the formation of autophagosomes whose presence was associated with enhanced viral replication, as shown by the use of Torin 1, a chemical inducer of autophagy or the specific autophagy inhibitor 3-Methyladenine. The results presented herein permit to gain better insight in the biology of ZIKV and to devise strategies aiming to interfere with the pathology caused by this emerging Flavivirus.

66 **IMPORTANCE**

67 Zika virus (ZIKV) is an arbovirus belonging to Flaviviridae family. Vector-mediated
68 transmission of ZIKV is initiated when a blood-feeding female *Aedes* mosquito injects the
69 virus into the skin of its mammalian host, followed by infection of permissive cells *via*
70 specific receptors. Indeed, skin immune cells, including dermal fibroblasts, epidermal
71 keratinocytes and immature dendritic cells, were all found to be permissive to ZIKV infection.
72 The results also show a major role for the phosphatidylserine receptor AXL as a ZIKV entry
73 receptor, and cellular autophagy in enhancing ZIKV replication in permissive cells. ZIKV
74 replication leads to activation of an antiviral innate immune response and the production of
75 type I interferons in infected cells. Taken together, these results provide for the first time a
76 general insight into the interaction between ZIKV and its mammalian host.
77

INTRODUCTION

Zika virus (ZIKV) is a little known emerging mosquito-borne Flavivirus, belonging to the Flaviviridae family that is closely related to the Spondweni serocomplex. Like other members of the Flavivirus genus, ZIKV contains a positive single-stranded genomic RNA, encoding a polyprotein that is processed into three structural proteins, the capsid (C), the precursor of membrane (prM) and the envelope (E), and seven nonstructural proteins NS1 to NS5 (1). Virus replication occurs in the cellular cytoplasm.

Epidemiological studies point out to a wide-spread distribution of ZIKV in the northern half of the African continent, as well as in many countries in south-east Asia, including Malaysia, India, the Philippines, Thailand, Vietnam, Indonesia, and Pakistan (2-9). Many different mosquito *Aedes* species can account for the transmission of ZIKV, including *Ae. aegypti* (10, 11) which is at present considered to be the main vector of the virus in South and South-East Asia, (11, 12). The first human ZIKV infection has been reported in Uganda in 1964 (2, 3, 5, 13) and the virus was later isolated from humans in South East Asia (8, 14-16). Despite this broad geographical distribution, human ZIKV infections have remained sporadic and limited to small-scale epidemics for decades, until 2007 when a large epidemic was reported on Yap Island, a territory of the Federated States of Micronesia, with nearly 75% of the population being infected with the virus (17). Moreover, an outbreak of a syndrome due to Zika fever has been reported in French Polynesia, in addition to several cases of ZIKV infection in New Caledonia, Easter Island and the Cook Islands, indicating a rapid spreading of the virus in the Pacific (18). Also, two imported cases of ZIKV infection of travellers from Indonesia and the Cook Islands, respectively, to Australia and two from Thailand to Europe and Canada, respectively have been described recently (19-22), emphasizing the capacity of ZIKV to spread to non-endemic areas where the proper mosquito vector might be present. The largest outbreak of ZIKV ever reported was characterized by fever, rash, arthralgia and conjunctivitis

in infected individuals. Moreover, during the recent outbreak in French Polynesia, ZIKV infection-related neurological disorders were also described and the incidence of Guillain Barré syndrome unexpectedly increased by 20 fold (23). In absence of monkeys in French Polynesia, it is likely that humans served as primary amplification hosts for ZIKV.

Because ZIKV has received far less attention than other emerging arboviruses such as Yellow fever, dengue (DENV), West Nile (WNV), Japanese encephalitis and Chikungunya viruses, pathogenesis of ZIKV infection remains still poorly understood. Mosquito-mediated transmission of ZIKV is initiated when a blood-feeding female *Aedes* mosquito injects the virus into the human skin followed by infection of permissive cells (reviewed in (24)). However, no information is available, neither on the nature of the skin cells that are permissive to infection with ZIKV, nor on the entry receptor used by this Flavivirus. Moreover, the mechanisms of ZIKV infection, the signaling pathways and the anti-viral immune response of the host, elicited by this virus, remain to be determined. In the present study, we describe the entry receptors and cellular targets of the most recent ZIKV isolate, responsible for the recent epidemic in French Polynesia, to provide a general insight into the interaction between this virus and its human host.

MATERIELS AND METHODS

Ethics Statement

The study was approved by the IRD ethics committee (registration number: AC-2013-1754) and all donors gave written informed consent.

Cells, virus and reagents

Ae. albopictus C6/36 cells, used for propagation of the ZIKV strain were grown in DMEM (Invitrogen, Cergy Pontoise, France), supplemented with 10% fetal calf serum (FCS, Lonza,

Basel, Switzerland) at 28°C**,** as previously described (25). Primary human dermal fibroblasts were obtained from neonatal foreskins and cultured at 37°C, 5% CO_2, in Fibroblast Basal Medium-2, supplemented with FGM-2 supplements and growth factors (all purchased at Lonza). The HFF-1 skin fibroblast cell line, HEK293T, A549 and Vero cells were maintained in DMEM supplemented with 10% FCS. HEK293T cells stably expressing DC-SIGN, TIM-1, TIM-4, AXL or Tyro3 have been reported previously (26). Primary human epidermal keratinocytes were obtained from neonatal foreskins (Lonza, Basel, Switzerland) and cultured at 37 °C, 5% CO_2, in Keratinocyte Basal Medium-2 (Lonza, Basel, Switzerland) supplemented with KGM-2 supplements and growth factors (Lonza, Basel, Switzerland). Low-passaged PF-25013-18 strain of ZIKV (a generous gift of VM. Cao-Lormeau and D. Musso ; ILM, Tahiti island, French Polynesia) isolated from a viremic patient in French Polynesia in 2013, was used in the current study and grown in mosquito *Ae. albopictus* C6/36 cells. The DENV-2 Jamaica/N.1409 strain (GenBank: M20558.1) was propagated in AP61 cell monolayers after having undergone limited cell passages. Recombinant human IFN-α, IFN-β, IFN-γ and Torin 1 autophagy inducer were purchased from R&D Systems (Lille, France). The autophagy inhibitor 3-MA was purchased from Sigma.

Dendritic Cell Generation

Human peripheral blood mononuclear cells were isolated from healthy donors by density centrifugation over Ficoll-Paque Plus (Amersham Biosciences, France). Monocytes were negatively selected with magnetic beads coated with a mixture of antibodies (Miltenyi Biotec, France) and seeded at 10^6 cells/ml in RPMI 1640 supplemented with 10% FCS, 1% penicillin/streptomycin, 50 ng/ml recombinant human interleukin-4 (PeproTech, France), and 100 ng/ml recombinant human granulocyte macrophage colony-stimulating factor (PeproTech, France) for 7 days.

ZIKV infection of cells

For infection, cells were seeded in culture plates at 4.10^4 cells per cm^2. Then, cells were rinsed once with PBS and the ZIKV diluted to the desired MOI was added to the cells. The cells were incubated for 2 h at 37°C with gentle agitation every 30 min. Next, the inoculum was removed and the cells were washed twice with PBS. Culture medium was added to each well and the cells were incubated at 37 C, 5% CO_2 for the duration of the experiment. As a control, fibroblasts were incubated with culture supernatant from uninfected C6/36 cells, referred to in the present study as mock-infected cells.

ZIKV infection of human skin biopsies

Fresh, sterile human skin biopsies with a size of 88 mm were obtained from three adult healthy donors (age range: 38-43 years) following abdominoplastic surgery. The skin explants were cultured, as described by Limon-Flores et al (27). For infection, 10^6 PFU in a final volume of 50 µl DMEM were injected per biopsy. As a control, skin biopsies were injected with culture supernatant from uninfected C6/36 cells in a final volume of 50 µl DMEM. At different time points, the biopsies were harvested and soaked with enzymes which degrade the extracellular matrix by using the whole skin dissociation kit (Miltenyi Biotec, Paris, France). In a second step, single-cells were freed from the extracellular matrix by using the gentleMACS™ Dissociator (Miltenyi Biotec, Paris, France) and cells were lysed with TriREAGENT (Sigma, Saint Quentin Fallavier, France) for RT-PCR analysis. For histological analysis biopsies were fixed in neutral-buffered formalin and embedded in paraffin. Tissue sections (3-5 µm) were stained with hematoxilin-eosin, put on slides and digitalized with Nanozoomer scanner (Hamamatsu, Massy, France) with a 20x objective.

Journal of Virology

ZIKV real-time RT-PCR

Total RNA was extracted from human fibroblasts using TriREAGENT (Sigma, Saint Quentin Fallavier, France) according to manufacturer's protocol. The RNA pellet was resuspended in 30 µL of RNAse free distilled water and stored at 80°C. 1µg was used for reverse transcription using M-MLV Reverse Transcriptase (Promega, Charbonnieres, France) according to manufacturer's instruction. The Maxima™ Probe/ROX qPCR Master Mix (Fermentas, Saint Remy les Chevreuses, France) was used in all qPCRs. Each reaction of 25 µL contained 500 nM of forward primer, 500 nM of reverse primer 250 nM of specific probe and 1x Maxima™Probe/ROX qPCR Master Mix as final concentration. Primers and probe sequence targeted ZIKV were already described (28). Amplification in an Applied Biosystem 7300 real-time PCR system involved activation at 95 C for 10 min followed by 40 amplification cycles of 95° C for 15 s, 60 C for 15 s and 72 C for 30 s. Real-time data were analyzed using SDS software from Applied. Viral RNA was quantified by comparing the sample's threshold cycle (Ct) values with a ZIKV virus RNA standard curve which was obtained as follows: firstly, total viral RNA from the cell culture was purified using QIAamp Viral RNA kit (Qiagen, Courtaboeuf, France) following the manufacturer's protocol. Then, standard RT-PCR was carried out by using a primer containing the T7 promoter sequence (T7-ZIKV_F-TAATACGACTCACTATAGGGTTGGTCATGATACTGCTGATTGC, ZIKV_R- CCTTCCACAAAGTCCCTATTGC). The PCR product was used to generate ZIKV RNA fragments by *in vitro* transcription using the MAXIscript kit (Ambion, Austin Texas, USA). Then, RNA was purified by ethanol precipitation. RNA strands generated were determined by spectrophotometry and converted to molecular copies using the following formula:

$$Ymolecules \quad /\mu L \;=\; \frac{Xg \;/\mu LRNA}{transcript \quad lenght \quad (bp) \times 340} \times 6.02 \times 10^{23}$$

RNA standards containing RNA copies were used to construct a standard curve.

Real-time PCR analysis

cDNA was synthesized using 2 µg RNA and MMLV reverse transcription kit (Promega, Charbonière, France), following the manufacturer's protocol. Gene expression was quantified using real-time PCR with the Applied Biosystem 7300 real-time PCR system. Real-time PCR was performed using 2 µl of cDNA with specific primers targeting the genes of interest (Table S1) and 10 µl of Maxima™ Sybr/ROX qPCR Master Mix (Fermentas, Saint Remy les Chevreuses, France) in a final reaction volume of 20 µl. The cycling conditions were 45 cycles of 95° C for 15 s, 60 °C for 15 s, and 72 °C for 30 s. mRNA expression (fold induction) was quantified by calculating 2-ΔΔCT with GAPDH mRNA as an endogenous control.

RT2 Profiler PCR Array

Total RNA was extracted from primary human skin fibroblasts, using TriReagent (Sigma, Saint Quentin Fallavier, France), according to the manufacturer's instructions. The concentrations of all RNA samples were assessed using the NanoDrop spectrophotometer (NanoDrop Technologies, Wilmington, DE). The same amount of total RNA (400 ng) from each sample was subjected to a cDNA synthesis reaction using the RT2 First Strand Kit (Qiagen, Valencia, CA). The resulting cDNA reaction (20 µL per sample) was diluted in 91 µl of nuclease-free H_2O (Qiagen). The diluted cDNA (102 µL) was mixed with 1248 µl of H_2O plus 1350 µL of 2x RT^2 SYBR green RT^2 Master Mix. The cocktail was dispensed at 10 µl per well into the 384-well RT2 Profiler PCR Array plate for profiling a total of 84 genes, as described in the manufacturer's handbook (PAHS-122Z, SABiosciences, Frederick, MD). Five Housekeeping genes (ACTB, B2M, GAPDH, HPRT1 and RPL13A) were used an an

internal control. DNA amplification was carried out with the Roche LightCycler 480 real-time cycler using a two-step cycling program: 95°C for 10 min, followed by 40 cycles of 95° C for 15 sec and 60° C for 1 min followed by a melting curve acquisition step. The resulting threshold cycle values for the plate were exported to a blank Excel work sheet. An automatic datasheet for analysis was downloaded from the SABiosciences Web portal (www.SABiosciences.com/pcrarraydataanalysis.php). The fold changes of gene expression were calculated in comparison to the values of controls:

$$fold\ \ change = 2^{-(\Delta Ct_{experiment} - \Delta Ct_{control})}$$

in which DCt =Ct (the gene of interest) - (the housekeeping gene), where Ct is the cycle threshold. The average of reverse-transcription controls and positive PCR control cycle threshold (Ct) values was used to normalize gene expression and determine fold change between groups. To evaluate gene expression, we selected the fold change on the basis of the criteria of at least a 2-fold up- or downregulation, as compared with the mock-infected cells. Gene regulation was considered statistically significant at a 95% confidence level (p value 0.05). The confidence level was determined from the data obtained from each sample in triplicate. Statistical analysis was performed using the RT^2 profiler RT-PCR Array Data Analysis version 3.5.

Immunolabeling

Twenty-four and 48 h following infection of fibroblasts, ZIKV infected and mock-infected cells were fixed with 3.7% paraformaldehyde in PBS for 1h at room temperature. Slides were blocked with an incubation in 10% FCS and 0.3% Triton X-100 for 30 min and incubated for 2 h at 37° C with the monoclonal antibody (mAb) 4G2 which is directed against the flavivirus

envelope protein. Cells were washed with PBS and incubated for 60 min at room temperature with a FITC-conjugated anti-mouse IgG. Hoechst 33258 dye was used to stain the nucleus. Preparations were examined with a Zeiss Apotome/Axioimager device. Autophagy was monitored after fixation of the cells in a 3.7% paraformaldehyde-PBS solution for 10 min at room temperature, permeabilization and labelling with anti-LC3 mAbs (Sigma). Coverslips were and analyzed by epifluorescence using a Leica microscope.

Electron Microscopy

Primary human fibroblasts were exposed to ZIKV at a MOI 10 cultured at 5% CO_2 for 72 h, collected, washed twice with PBS and fixed for 1h at 4 °C in a solution containing 2.5 % glutaraldehyde in 0.1 M cacodylate buffer pH 7.4. Cells were then rinsed three times in cacodylate buffer and post-fixed for 1 h with 1% OsO4 (Electron Microscopy Sciences Inc.). After an additional washing, the cells were incubated for 30 min in 0.5% tannic acid (Merck). Dehydratation was obtained with a graded series of ethanol solutions (from 25 to 100%) before embedding in Epok resin at 60 °C for 48h (Electron Microscopy Sciences Inc.). Ultrathin sections were cut with a Reichert Ultracut microtome (Leica) and then examined under a Hitachi H7100 transmission electron Microscope at 75kV.

ZIKV Plaque Assay

Four different 10-fold dilutions of purified virus were spread onto monolayers of VERO cells at 37° C for 2 h to initiate binding to cells. Then, a mix of nutriment solution with agar (Lonza) was added. The cells were maintained at 37°C for 6 days before the plaque assay. For plaque counting, the cells were incubated with 3.7 % formaldehyde and 0.1% Crystal violet in 20% ethanol. This experiment was repeated three times.

Western blotting analysis

Cells were lysed on ice in RIPA buffer (150 mM NaCl, 5 mM β-mercaptoethanol, 1% NP-40, 0.1% sodium dodecyl sulfate, 50 mM Tris- HCl pH 8), supplemented with complete protease inhibitor cocktail solution (Sigma). Protein concentration was determined by BCA assay (ThermoScientific, Saint Herblain, France). Equal amounts of proteins were mixed with Laemmli sample buffer, subjected to SDS-PAGE and electrotransferred onto a nitrocellulose membrane. The membrane was blocked with PBS 0.05% Tween-20, containing 5% skimmed milk, incubated overnight at 4°C with anti-MX1 as a primary antibody, washed three times with PBS-Tween and subsequently incubated for 1h at RT with horseradish peroxidase-coupled secondary antibodies in PBS-Tween, containing 1% skimmed milk. The membrane was washed three times and proteins were detected by chemiluminiscence, using the SuperSignal West Pico Chemiluminescent Substrate kit (ThermoScientific). The immunoblot was then stripped and reblotted with an anti-α-tubulin Ab to ensure that equivalent levels of protein were loaded in each lane.

Flow Cytometry Analysis

Flow cytometry analysis was performed as previously described (26). ZIKV infection was detected using the anti-4G2 mAb.

Inhibition of Infection Assay

Cells were incubated for 30 min prior to infection with media containing the indicated quantities of goat anti-TIM and/or anti-AXL polyclonal antibodies. Identical concentrations of purified normal goat IgG were used as control. Cells were then infected with ZIKV or DENV for 3 hr incubation in the presence of inhibitors, washed and incubated with culture medium. Infection was quantified by flow cytometry.

RNA Interference

Cells were transiently transfected using the Lipofectamine RNAiMax protocol (Life Technologies) with 10 nM final siRNAs (26). After 48 hr, cells were infected at the indicated MOI, and infected cell percentages were quantified 24 hr postinfection by flow cytometry. For PRR signaling pathways, 50 nM final siRNAs were used. Pools of siRNAs (ON-TARGETplus SMARTpool) used in this study were from Dharmacon: TIM-1 (L-019856-00), AXL (L-003104-00), TLR3 (L-007745-00), TLR7 (L004714-00), RIG-I (L-012511-00), MDA5 (L-013041-00). A non-targeting pool (NT) was used as a negative control.

RESULTS

Human skin cells are permissive for ZIKV infection and replication

Given the capacity of mosquitoes to inoculate ZIKV into the human skin during the blood feeding process, the potential target cells for infection with this virus are likely to be localized in the epidermis and dermis which also constitute the first line of defense. We first determined ZIKV susceptibility of skin fibroblasts, that have been recognized as a permissive target for various arboviruses. Cells were infected *in vitro* with ZIKV and the presence of viral envelope antigens was evaluated by immunofluorescence at different hours post infection (hpi). No staining was observed in mock-infected cells or cells stained with an isotype control antibody (Figure 1A). In contrast, as soon as 24h post-infection (hpi), the viral envelope protein was detected in several cells, whereas at 72 hpi 100% of the infected cells expressed ZIKV (Figure 1A). Next, we evaluated the ability of these cells to produce viral progeny *in vitro* by determining viral titers in the supernatants of ZIKV-infected primary human skin fibroblasts using a standard plaque assay. The results show a gradual increase in the production or viral particles over time indicating active viral replication in the infected cells (Figure 1B).

Intracellular viral RNA was also quantified by real time PCR at different time points post-infection. ZIKV RNA was detected in fibroblasts challenged with the virus, but not in mock-infected cells, as shown in Figure 1C. Viral RNA copy numbers were detected as soon as 6 hpi and increased during the course of infection. The amount of viral transcripts was markedly high and could reach 10^8 RNA copies per microliter in cells infected with ZIKV and maintained in culture for 24-48 h.

Then, given the observation that the epidermis layer is comprised mainly of keratinocytes, we hypothesized that the latter cells also could be a target for ZIKV. Primary human epidermal keratinocytes obtained from neonatal foreskin were infected with ZIKV and intracellular viral RNA was quantified by quantitative PCR at different time points post-infection. As shown in Figure 2A, ZIKV mRNA was detected in keratinocytes challenged with ZIKV, but not in mock-infected cells. Viral RNA was found to increase over time and could be detected as soon as 6 hpi, with a maximal amount of 10^5 viral copies per ml at both 48 and 72 hpi. The capacity of ZIKV to replicate *ex vivo* in human skin cells was also studied. Infection of human skin explants with ZIKV resulted in a gradual increase in viral copy numbers, with maximal levels at 5 days post infection (dpi), pointing to a process of active viral replication (Fig. 2B). Histological analysis of mock-infected human skin explants showed all aspects of a normal healthy skin with a stratified epidermal layer, containing basal keratinocytes and differentiated layers consisting of stratum granulosum and stratum corneum, respectively (Figure 2C). In contrast, ZIKV-infected keratinocytes in human skin explants 5 dpi showed the appearance of a cytoplasmic vacuolation, as well as the presence of pyknotic nuclei which was however not generalized throughout the epidermis, but limited to the stratum granulosum (Figure 2D). Moreover, ZIKV infection induced the sporadic formation of edema which was also limited to this subcorneal layer (Figure 2E).

Immature dendritic cells have been reported to be permissive for DENV infection and as such are recognized as an important target for propagation of this virus in the human skin. ZIKV infection was therefore also investigated on this cell type, using DENV as a control, by analyzing the intracellular presence of the viral envelope protein by flow cytometry. Our results show that about 50% of human *in vitro* generated immature dendritic cells challenged with ZIKV at MOI 0.5 for 24 hpi expressed the viral envelope (Figure 3). This percentage was identical, as compared to that of the cells infected with DENV under the same experimental conditions. These results indicate that immature dendritic cells are also permissive to infection by this member of the Flavivirus family.

DC-SIGN, TIM and TAM receptors are involved in ZIVK infection

Several receptors, among which DC-SIGN, as well as certain TIM and TAM proteins, two members of the phosphatidylserine receptor family, have been reported to facilitate viral entry of DENV (review in (29)). To determine whether these receptors are also involved in ZIKV entry, a series of HEK293T cell transfectants, expressing DC-SIGN, TIM1, TIM4, or the TAM family members AXL and TYRO3, in a stable manner, were exposed to the virus. The expression levels of each of these receptors are shown in Figure 4A. The parental, non-transfected HEK-293T cells were not susceptible to ZIKV-infection, as shown by the absence of ZIKV antigen detection (Figure 4B). The expression of either DC-SIGN or AXL strongly enhanced viral infection, already at MOI 0.1, resulting in about 50% of ZIKV-infected cells. TYRO3-expressing HEK-293T cells were also highly permissive for ZIKV with nearly 70% of the cells infected with the virus at 24 hpi. In contrast, the expression of TIM-1 or TIM-4 had only modest or marginal effects on ZIKV entry (Figure 4B). To further determine the relative contribution of TIM and TAM receptors on ZIKV infection, A549 cells that

endogenously express TIM-1 and AXL, but not DC-SIGN (Figure 5A) were infected with the virus. In keeping with the potent ZIKV infection-inducing activity of AXL, a neutralizing Ab, specific for this receptor, strongly inhibited viral infection of A549 cells (Figure 5B). In contrast, the presence of a neutralizing anti-TIM1 Ab did not have an impact on the percentage of ZIKV infected cells at 24 hpi, as compared to cells infected with ZIKV alone. However, the combination of the anti-TIM-1 and anti-AXL Abs completely abrogated ZIKV infection (Figure 5B). We also used the RNA silencing technique to downregulate TIM-1 and/or AXL expression in A549 cells (Figure 5C). The results mirrored those obtained with the neutralizing Ab, in that ZIKV infection was only slightly reduced in TIM-1-silenced cells, strongly inhibited in AXL-silenced cells and totally abrogated when both genes were silenced (Figure 5D). Finally, to determine the importance of the AXL in ZIKV infection of human skin fibroblasts that express AXL but not TIM-1 (Figure 6A) were infected with the virus in the absence or presence of a neutralizing Ab or specific siRNA. Exposure of the human skin fibroblast cell line HFF1 to ZIKV, or DENV as a positive control, resulted in a comparable number of infected cells that was inhibited by 70% and 50%, respectively, in the presence of a neutralizing anti-AXL Ab (Figure 6B). Strikingly, the presence of specific AXL siRNA totally inhibited the AXL expression (Figure 6C) and effectively abrogated the infection with either virus, thus demonstrating the importance of AXL in the permissiveness of human skin fibroblasts to infection and replication of ZIKV. Taken together, the data indicate an essential and cooperative role for both TIM and TAM family members in ZIKV infection by permissive cells.

ZIKV induces an innate anti-viral response in primary human skin fibroblasts

In order to determine whether ZIKV induces an innate anti-viral immune response in permissive cells, the anti-viral gene expression profile in infected primary human fibroblasts at

Journal of Virology

399 early time points following ZIKV infection was determined using a human qPCR array
400 covering 84 human antiviral genes. This comparative analysis with mock-infected cells
401 showed the specific induction of pattern recognition receptors (PRRs), able to detect the
402 presence of pathogen-associated molecular patterns (PAMPs) in response to ZIKV infection.
403 This is particularly illustrated by the upregulation of the Toll-like receptor 3 (TLR-3) mRNA
404 expression, as well as by enhanced transcription of the DDX58 (RIG-I) and MDA5 (IFIH1)
405 genes that reportedly are involved in the detection of other Flavivirus members (Table 1).
406 Increased PRR expression levels and kinetics of expression, during an extended time course of
407 infection, were confirmed by individual qRT-PCR analysis. As shown in Figure 7A, RIG-I,
408 MDA5 and TLR3 expression was upregulated in ZIKV-infected fibroblasts as soon as 6 hpi
409 with maximal mRNA levels detected at 48 hpi. In contrast, no activation of the TLR7 gene
410 was observed in these cells following infection with ZIKV. The detection of viral PAMPs by
411 TLR3 and other PRRs initiates downstream signaling pathways that account for the
412 enhancement of transcription factors known to mobilize the antiviral machinery. The results
413 shown in Table 1 and Figure 7A are consistent with this general notion, as IRF7 mRNA levels
414 were increased in ZIKV-infected cells. IRF7 is a transcription factor that binds to the
415 interferon-stimulated response element, located on the promoters of type I IFN genes (30).
416 This result not only corroborates the enhanced IFN-α and IFN-β gene expression detected
417 following infection with ZIKV, but also the upregulation of the expression of several
418 interferon-stimulated genes (ISGs), including OAS2, ISG15 and MX1 (Table 1 and Figure
419 7B). The expression of the CXCR3 ligand CXCL10, as well as the inflammatory antiviral
420 chemokine CCL5, was also induced by ZIKV. Finally, ZIKV infection of skin fibroblasts was
421 also found to activate certain inflammasome components, as evidenced by a strong increase in
422 the expression of AIM2 and IL-1β transcripts (Figure 7A). In order to determine the
423 involvement of each of the upregulated PRRs in the anti-viral response against ZIKV, the

effect of specific siRNAs on viral replication was studied. Expression levels of MDA-5, RIG-I, TLR3 and TLR-7 in HFF1 cells were decreased by 80%, 24h following the transfection of these cells with specific siRNA, and were completely inhibited after 48h (Figure 8A-D), thus validating the efficacy of this approach. Inhibition of TLR3 expression, unlike that of the other PRRs, resulted in a strong increase in the viral RNA copy numbers 48h following viral infection of the cells (Figure 8E). However, inhibition of TLR3 expression did not modulate type I IFN mRNA expression in the infected cells (Results not shown). Taken together, these results underscore the importance of TLR3 in the induction of an antiviral response against ZIKV.

Type I and type II IFNs inhibit ZIKV replication

Because of the observed induction of type I IFNs by ZIKV-infected skin fibroblasts, their effects on viral replication in the latter cells was investigated. Primary skin fibroblasts were pretreated for 6h with increasing doses of recombinant human IFN-α, IFN-β or IFN-γ, infected with ZIKV at an MOI of 1, and viral RNA copy numbers were determined by real-time PCR. At this viral titer, both type I and type II IFNs strongly, and dose-dependently, inhibited viral replication with similar efficacy (Figure 9A-C). The effect of IFNs was corroborated by a decrease in the release of viral particles as measured by plaque assay in the culture supernatants of the infected cells (Fig. 9D-F). These results show that ZIKV is highly sensitive to the antiviral effect of both type I and type II IFNs.

Autophagosome formation in infected skin fibroblasts increase ZIKV replication

Autophagy is a multi-step process responsible for degradation and recycling of cytoplasmic components that augments the replication and dissemination of several arboviruses. We therefore analyzed whether infection of skin fibroblasts with ZIKV resulted in the formation of autophagosomes. First, an electron microscopy study was carried out to demonstrate the

presence of ZIKV particles in cytoplasmic compartments, as a result of exposure of these cells to the virus. At 72 hpi, intravacuolar structures in ZIKV-infected fibroblasts were found to contain capsids, in combination with enveloped and electron dense spherical viral particles that were 70 to 100 nm in diameter which is a general feature of Flavivirus particles (Figure 10A and 10B). Moreover, ZIKV infection was associated with the formation of numerous double-membrane intracytoplasmic vacuoles characteristic of autophagosomes (Figure 10C and 10D) that were not observed in mock-infected cells (results not shown). To further determine whether autophagy was induced following ZIKV infection, the skin fibroblast cell line HFF1 was infected with the virus and the co-expression of the viral envelope protein and the cytosolic microtubule-associated light chain 3 (LC3), an autophagosome-specific marker, was determined by confocal microscopy. Torin 1, a chemical inducer of autophagy was used as a positive control. As shown in Figure 11A, ZIKV infection induced the formation of LC3 punctae in infected fibroblasts while LC3 labelling was more diffuse in mock-infected cells. Interestingly, LC3 signal in infected cells completely co-localized with that of the viral envelope protein detected with specific antibodies. Moreover, the simultaneous addition of ZIKV and Torin 1 to primary fibroblasts enhanced viral replication as shown by an increase in the viral RNA copy number (Figure 11B). Conversely, addition of the 3-Methyladenine (3-MA) autophagy inhibitor decreased the number of viral copies in ZIKV-infected cells without any cytotoxic effect on the cells (results not shown), thus formally confirming the association between enhanced autophagosome formation and increased viral replication. Taken together, these results show that ZIKV is able to increase its replication *via* induction of the autophagy in the host cell.

Journal of Virology

DISCUSSION

ZIKV is a Flavivirus, related to Yellow fever, Dengue, West-Nile and Japanese encephalitis viruses, that causes an arthropod-borne disease in human known as ZIKA fever. Originally detected in a sentinel Rhesus monkey in Uganda in 1947 (31) and twenty years later isolated from humans in Nigeria, the virus has since spread to other regions of the world. Importantly, following recent outbreaks in Micronesia, French Polynesia, Cook Island and Easter Island, ZIKV has become an emerging arbovirus (18). However, other than its phylogenetic relationship to other members of the Flavivirus family, no information is available on the cellular tropism of ZIKV and the nature of the cellular receptors that mediate its entry. In the present study, we have identified the initial target cells of the ZIKV in the skin compartment, as well as its entry receptors, and have furthermore characterized the anti-viral response elicited following infection of permissive cells with the PF-13 ZIKV strain isolated during the recent outbreak in French Polynesia (18). This strain is closely related to those isolated from patients infected during the ZIVK outbreaks in Cambodia in 2010 and Yap State in 2007 and its thus relevant for the results reported here.

ZIKV is transmitted by the *Aedes* mosquito that deposits the virus in the epidermis and dermis of the bitten host during a blood meal. Indeed, both skin fibroblasts and epidermal keratinocytes were found to be highly permissive to infection with ZIKV. Infection of skin fibroblasts rapidly resulted in the presence of high levels of RNA copy numbers and a gradual increase in the production or ZIKV particles over time, indicating active viral replication in the infected cells.

ZIKV infection of epidermal keratinocytes resulted in the appearance of cytoplasmic vacuolation, as well as the presence of pyknotic nuclei in the stratum granulosum, indicative for cells that undergo apoptosis. This bears similarity to observations made with DENV that

induces the appearance of apoptotic cells in the epidermis of infected human skin explants (27). It can be speculated that the induction of apoptotic cell death is a mechanism by which ZIKV, like DENV, is able to divert anti-viral immune responses by increasing their dissemination from dying cells. These results also corroborate previous reports in the literature showing the importance of keratinocytes in infection with other flaviviruses, such as WNV (32) and DENV (25). In addition to dermal fibroblasts and epidermal keratinocytes, we report that dendritic cells are permissive to infection with ZIKV. This comes as no surprise given the involvement of skin antigen presenting cells in the replication of other flavivirus members, in particular DENV that efficiently infects Langerhans cells (33). The selective susceptibility of permissive cells in the dermis and epidermis, including Langerhans cells, dermal dendritic cells, macrophages, as well as fibroblast and keratinocytes, to infection with ZIKV needs however to be determined.

The first step of Flavivirus entry into a host cell is mediated by the viral envelope protein that interacts with several cell surface receptors and attachment factors, the differential expression of which determines the cellular tropism of the virus. At present, more than a dozen putative entry receptors and factors, in particular for DENV, have been described. Several of them, such as heat-shock proteins, laminin receptor, integrin αvβ3, prohibitin, claudin-1, scavenger receptor class B and natural killer cells receptor NKp44, can interact with viral particles in mammalian and/or mosquito cells, but their exact role in the flavivirus entry program, as well as their physiologic relevance, is not well understood (reviewed in (29). Heparan sulfate, a sulfated polysaccharide associated to proteins from the extracellular matrix, has been described as a non-specific attachment factor of flaviviruses, concentrating viral particles on the cell surface and facilitating their interaction with primary receptors (34-38). Among them, C-type lectin receptors such as the dendritic cell-specific intracellular adhesion molecule 3-grabbing non-integrin (DC-SIGN, CD209), the mannose receptor and the C-type lectin

522 domain family 5, member A (CLEC5A, MDL-1), play an important role in flavivirus binding
523 and infection of myeloid cells (39-41). Recently, TIM and TAM proteins, two distinct
524 families of transmembrane receptors that participate in the phosphatidylserine (PtdSer)-
525 dependent phagocytic engulfment and removal of apoptotic cells, have also been shown to act
526 as DENV entry factors, promoting viral infection by attaching and possibly internalizing viral
527 particles in human cell cultures and primary cells targeted by flaviviruses (26, 29).
528 We show here that ZIKV entry is mediated by DC-SIGN, AXL, Tyro3 and, although to a
529 lesser extent, by TIM-1. Although TIM-1 by itself contributed little to ZIKV infection, its
530 expression nevertheless had an additive effect on the efficacy of AXL-mediated viral entry.
531 This raises the interesting possibility of a cooperation between both receptors, with TIM-1
532 acting as an attachment factor that binds viral particles and transfers them to AXL which
533 could in turn participate in viral internalization. In that sense, TIM-1 might not be
534 indispensable for ZIKV endocytosis and infection, but would rather concentrate virions on the
535 cell surface to facilitate their interaction with AXL, as well as the subsequent infection, which
536 might explain the additive inhibitory effect observed when both receptors are blocked with
537 neutralizing antibodies. However, additional experiments are required to assess the exact role
538 played by TIM and TAM receptors in ZIKV infection.
539 As has been reported for DENV, there seems to be a large number of receptors and/or
540 attachment factors that are able to mediate entry of ZIKV in permissive cells. It is of note
541 however that the permissiveness of skin cells to ZIKV is also determined by the profile of
542 receptor expression by these target cells. In this respect, unlike immature dendritic cells that
543 also are a primary target cell type for ZIKV infection, neither cutaneous fibroblasts, nor
544 epidermal keratinocytes express DC-SIGN. In contrast, the latter cells, as well as
545 macrophages, vascular endothelium cells and astrocytes (reviewed in ref (42), express AXL
546 that, as shown in the present study, is of major importance for ZIKV entry. The availability of

different entry receptors is likely to provide an evolutionary advantage for the virus that, as a result, is able to infect a wide range of target cells and invade the human host. Nevertheless, the contribution of each of these receptors and/or attachment factors to ZIKV infection and pathogenesis is currently unknown and remain to be established. It is also important to consider that other, as yet to be identified cell surface molecules exist that might account for the tropism of ZIKV.

The outcome of viral infection is determined by a competition between viral replication and the host immune response. The latter is programmed to rapidly control viral replication and to limit virus spread by recognizing non-self nucleic acid as pathogen-associated molecular patterns and triggering an antiviral response. Indeed, infection of fibroblasts *in vitro* with ZIKV strongly induced the expression of several antiviral gene clusters, in particular PRRs, such as RIG-I, MDA-5 and TLR3 that are able to detect the presence of PAMPs. These results corroborate previous reports in the literature showing that these gene products play a sensory role in the detection of other flaviviruses, such as DENV and WNV (25, 43). The induction of TLR3 expression is rapid and already detectable at 6 hpi, whereas that of RIG-I and MDA-5 is delayed. It can therefore be hypothesized that these molecules trigger a coordinated induction of the antiviral immune reaction against ZIKV with TLR3 priming an early response that is amplified by RIG-I and MDA-5 at a later stage. This sequence of events has also been suggested previously with respect to the immune response of fibroblasts following infection with DENV (44). However, in the latter study, the involvement of only TLR3 and RIG-I was considered, because, contrary to ZIKV, DENV infection did not enhance the expression of MDA5 in skin fibroblasts.

Both TLR3 and TLR7 are implicated in the induction of an immune response against flavivirus and triggering of these PRRs has been shown to initiate signaling pathways, leading to the production of type I IFNs, as well as other inflammatory cytokines and chemokines by

hepatocytes and macrophages (review in (45). Indeed, ZIKV infection strongly enhanced TLR3 expression, associated with the production of IFN-α and IFN-β in infected cells. However, whereas inhibition of TLR3 expression by siRNA indeed resulted in a strong enhancement of viral replication, no effect on type I IFN mRNA expression was detected. Although TLR3 seem to play an important in role in the antiviral response to ZIKV, the mechanism by which this receptor contributes to the control of viral replication remains to be determined. In contrast, no modulation of TLR7 expression was observed, which is reminiscent to results obtained with DENV-infected skin fibroblasts (44). The absence of TLR7 induction was also reported in a separate study in which expression of PRRs in virally-infected fibroblasts of different origin was analyzed (46). Taken together, these findings confirm the notion that the involvement of various TLR members seems to be dependent on virus and cell type.

The detection of ZIKV-expressed PAMPs also resulted in an increase in transcriptional levels of IRF7, a transcription factor that binds to the interferon-stimulated response element, located on the promoters of type I IFN genes (30). This result corroborates the enhanced IFN-α and IFN-β gene expression, detected following infection with ZIKV, as well as the upregulation of the expression of several interferon-stimulated genes, including OAS2, ISG15 and MX1. The expression of the two CXCR3 ligands, CXCL10 and CXCL11 was also induced by ZIKV. The latter chemokines not only play a role in innate and adaptive immunity by attracting T cells and other leukocytes to sites of inflammation, but also display direct, receptor-independent, defensin-like antimicrobial activity when present at elevated concentrations in dermal fibroblasts (47). In addition, infection of skin fibroblasts by ZIKV resulted in upregulation of CCL5, another inflammatory chemokine known for it antiviral activity.

Whereas TLR3 transcription was significantly enhanced, IRF3 gene expression, in contrast, remained unchanged during the course of ZIVK infection of fibroblasts. A similar observation was made in DENV-infected epidermal keratinocytes in which also no enhanced IRF3 expression could be detected. This is somewhat surprising in that IFR3 is known to play an important role in the induction of IFN-β production in cells exposed to PAMPS from various viruses (48). Moreover, dsRNA-mediated triggering of RIG-I and MDA5, both molecules whose expression is upregulated following infection with ZIKV and other flaviviruses, seems to be crucial for IRF3 activation (25). It has been reported that IFN-β production, which is essential for the early antiviral immune response, was observed in both wild-type and IRF3-/- mice following WNV infection (48). These results corroborate the present and previously published data (25), indicating that the production of the type I IFN in response to DENV and ZIKV infection is apparently independent of the IRF3 pathway, both in flavivirus-infected epidermal keratinocytes and skin fibroblasts. It is of note that the replication of ZIKV was significantly inhibited by both type I and type II IFNs, in keeping with the general antiviral activity of these cytokines with critical functions in host defense mechanisms.

Electron microscopy analysis of ZIKV-infected primary skin fibroblasts showed the presence of membrane vesicles with a size between 70 and 100 nm that were located in intimate association with the endoplasmic reticulum, indicating that ZIKV replication occurs in close association with host cell membranes. These results are in line with an earlier report in the literature underscoring the importance of fibroblasts as a primary cell type of replication for flaviruses, like DENV, that through the release of viral particles may contribute to subsequent viral dissemination (44). ZIKV infection also induced an autophagy program, as demonstrated by the presence of characteristic autophagosome-like vesicles in the infected fibroblasts. Autophagy is a process characterized by the presence of double-membrane vesicles, known as autophagosomes, that recruit cytoplasmic material and subsequently fuse with lysosomes for

protein degradation. Autophagy not only participates in the degradation of proteins and damaged organelles in the cytoplasm to maintain homeostasis (49), but is also involved in host immunity against pathogen infection. This is particularly illustrated by Vesicular stomatitis virus (50), Sendai virus (51), and Herpes simplex virus-1 (52) infected cells in which, autophagy-mediated degradation of viral proteins limits viral replication and promotes cell survival. In contrast, the autophagy process can be subverted by viruses. This is true for several arboviruses, including DENV (53, 54), Chikungunya virus (55) and Japanese encephalitis (56) virus that use components of the autophagy pathway to promote their replication and dissemination by clearing cells through multiple mechanisms. In this regard, autophagy may thus have both pro- and antiviral effects.

Autophagy in ZIKV-infected fibroblasts was furthermore confirmed by the demonstration of co-localization of the viral envelope protein and the cytosolic microtubule-associated molecule LC3. The results also show that stimulation of autophagosome formation by Torin 1 further enhances replication of ZIKV in permissive cells, whereas the presence of 3 M-A, an inhibitor of autophagosome formation, strongly reduced viral copy numbers in the infected fibroblasts, indicating that autophagy promotes replication of ZIKV in permissive cells. In this respect, ZIKV behaves like most other flavivirus members, with the exception of WNV (57), by its capacity to interact with the conventional autophagy pathway in mammalian cells. The precise mechanism by which ZIKV induces autophagy still needs to be determined. Nevertheless, similar to DENV (58), the results from our study demonstrating the co-localization of ZIKV with LC3 strongly suggests that autophagocytic vacuoles are the site of viral replication. It can furthermore speculated that autophagy may promote replication of ZIKV infection through restriction of the antiviral innate immune response (59), enhancement of translation of the viral genome that has entered the mammalian cells (60) or by providing additional energy and relevant membrane structures for viral replication (61). However, the

exact molecular mechanism(s) by which ZIKV highjacks components of the autophagome pathways remain to be determined.

At present, ZIKV has received far less attention in the literature than the other mosquito-borne flavivirus members. Nevertheless, it is considered to be an emerging virus because of its global spreading during the last decades and its pathogenic potential reminiscent to that of DENV. Importantly, ZIKV has recently been isolated in Gabon from the Asian tiger mosquito *Ae*. *albopictus* (62), a rapidly expanding *Aedes* species that lives in close contact with human urban populations (63, 64) and that typically feeds not only at dusk and dawn, but also in the daytime. This underscores its menacing character, as this vector is known for its capacity to colonize new environments, either by progressive extension from already occupied zones, or by jumping to new areas, in particular to those in heavily populated urban areas. In this respect, a better understanding of the role of mosquito saliva in ZIKV infection is an important point that must be addressed in the future as well.

Taken together, the results presented in this study pertaining to the identification of the cellular tropism, molecular mechanisms of infection and replication, as well as signaling pathways involved the anti-viral immune response of ZIKV, permit to gain better insight in its mode of action and to devise strategies aiming to interfere with the pathology caused by this emerging flavivirus.

ACKNOWLEDGMENTS

The authors thank Dr François Renaud for critical discussions, Chantal Cazevieille for expert help with electron microscopy and Eric Bernard for technical assistance. This work was supported by grants from the French Research Agency “Agence Nationale de la Recherche” (ANR-12-BSV3-0004-01; ANR-14-CE14-0029). Sineewanlaya Wichit was supported by a

fellowship of the Infectiopôle Sud foundation. The funders had no role in study design, data collection and analysis, decision to publish, or preparation of the manuscript.

REFERENCES

1. **Kuno G, Chang GJ, Tsuchiya KR, Karabatsos N, Cropp CB.** 1998. Phylogeny of the genus Flavivirus. J Virol **72:**73-83.
2. **Moore DL, Causey OR, Carey DE, Reddy S, Cooke AR, Akinkugbe FM, David-West TS, Kemp GE.** 1975. Arthropod-borne viral infections of man in Nigeria, 1964-1970. Ann Trop Med Parasitol **69:**49-64.
3. **Simpson DI.** 1964. Zika Virus Infection in Man. Transactions of the Royal Society of Tropical Medicine and Hygiene **58:**335-338.
4. **Smithburn KC.** 1954. Neutralizing antibodies against arthropod-borne viruses in the sera of long-time residents of Malaya and Borneo. American journal of hygiene **59:**157-163.
5. **Fagbami AH.** 1979. Zika virus infections in Nigeria: virological and seroepidemiological investigations in Oyo State. The Journal of hygiene **83:**213-219.
6. **Hammon WM, Schrack WD, Sather GE.** 1958. Serological survey for a arthropod-borne virus infections in the Philippines. Am J Trop Med Hyg **7:**323-328.
7. **Pond WL.** 1963. Arthropod-Borne Virus Antibodies in Sera from Residents of South-East Asia. Transactions of the Royal Society of Tropical Medicine and Hygiene **57:**364-371.
8. **Olson JG, Ksiazek TG, Suhandiman, Triwibowo.** 1981. Zika virus, a cause of fever in Central Java, Indonesia. Transactions of the Royal Society of Tropical Medicine and Hygiene **75:**389-393.
9. **Darwish MA, Hoogstraal H, Roberts TJ, Ghazi R, Amer T.** 1983. A sero-epidemiological survey for Bunyaviridae and certain other arboviruses in Pakistan. Trans R Soc Trop Med Hyg **77:**446-450.
10. **Marchette NJ, Garcia R, Rudnick A.** 1969. Isolation of Zika virus from Aedes aegypti mosquitoes in Malaysia. Am J Trop Med Hyg **18:**411-415.
11. **Li MI, Wong PS, Ng LC, Tan CH.** 2012. Oral susceptibility of Singapore Aedes (Stegomyia) aegypti (Linnaeus) to Zika virus. PLoS Negl Trop Dis **6:**e1792.
12. **Boorman JP, Porterfield JS.** 1956. A simple technique for infection of mosquitoes with viruses; transmission of Zika virus. Transactions of the Royal Society of Tropical Medicine and Hygiene **50:**238-242.
13. **Monlun E, Zeller H, Le Guenno B, Traoré-Lamizana M, Hervy JP, Adam F, Ferrara L, Fontenille D, Sylla R, Mondo M.** 1993. [Surveillance of the circulation of arbovirus of medical interest in the region of eastern Senegal]. Bull Soc Pathol Exot **86:**21-28.
14. **Weinbren MP, Williams MC.** 1958. Zika virus: further isolations in the Zika area, and some studies on the strains isolated. Transactions of the Royal Society of Tropical Medicine and Hygiene **52:**263-268.

15. **Haddow AJ, Williams MC, Woodall JP, Simpson DI, Goma LK.** 1964. Twelve Isolations of Zika Virus from Aedes (Stegomyia) Africanus (Theobald) Taken in and above a Uganda Forest. Bulletin of the World Health Organization **31:**57-69.
16. **Haddow AD, Schuh AJ, Yasuda CY, Kasper MR, Heang V, Huy R, Guzman H, Tesh RB, Weaver SC.** 2012. Genetic characterization of Zika virus strains: geographic expansion of the Asian lineage. PLoS Negl Trop Dis **6:**e1477.
17. **Duffy MR, Chen TH, Hancock WT, Powers AM, Kool JL, Lanciotti RS, Pretrick M, Marfel M, Holzbauer S, Dubray C, Guillaumot L, Griggs A, Bel M, Lambert AJ, Laven J, Kosoy O, Panella A, Biggerstaff BJ, Fischer M, Hayes EB.** 2009. Zika virus outbreak on Yap Island, Federated States of Micronesia. The New England journal of medicine **360:**2536-2543.
18. **Musso D, Nilles EJ, Cao-Lormeau VM.** 2014. Rapid spread of emerging Zika virus in the Pacific area. Clin Microbiol Infect **20:**O595-596.
19. **Kwong JC, Druce JD, Leder K.** 2013. Zika virus infection acquired during brief travel to Indonesia. Am J Trop Med Hyg **89:**516-517.
20. **Tappe D, Rissland J, Gabriel M, Emmerich P, Gunther S, Held G, Smola S, Schmidt-Chanasit J.** 2014. First case of laboratory-confirmed Zika virus infection imported into Europe, November 2013. Euro surveillance : bulletin Europeen sur les maladies transmissibles = European communicable disease bulletin **19**.
21. **Pyke AT, Daly MT, Cameron JN, Moore PR, Taylor CT, Hewitson GR, Humphreys JL, Gair R.** 2014. Imported zika virus infection from the cook islands into australia, 2014. PLoS currents **6**.
22. **Fonseca K, Meatherall B, Zarra D, Drebot M, MacDonald J, Pabbaraju K, Wong S, Webster P, Lindsay R, Tellier R.** 2014. First case of zika virus infection in a returning canadian traveler. Am J Trop Med Hyg **91:**1035-1038.
23. **Oehler E, Watrin L, Larre P, Leparc-Goffart I, Lastere S, Valour F, Baudouin L, Mallet H, Musso D, Ghawche F.** 2014. Zika virus infection complicated by Guillain-Barre syndrome--case report, French Polynesia, December 2013. Euro surveillance : bulletin Europeen sur les maladies transmissibles = European communicable disease bulletin **19**.
24. **Briant L, Desprès P, Choumet V, Missé D.** 2014. Role of skin immune cells on the host susceptibility to mosquito-borne viruses. Virology **464-465:**26-32.
25. **Surasombatpattana P, Hamel R, Patramool S, Luplertlop N, Thomas F, Despres P, Briant L, Yssel H, Misse D.** 2011. Dengue virus replication in infected human keratinocytes leads to activation of antiviral innate immune responses. Infection, genetics and evolution : journal of molecular epidemiology and evolutionary genetics in infectious diseases **11:**1664-1673.
26. **Meertens L, Carnec X, Lecoin MP, Ramdasi R, Guivel-Benhassine F, Lew E, Lemke G, Schwartz O, Amara A.** 2012. The TIM and TAM families of phosphatidylserine receptors mediate dengue virus entry. Cell Host Microbe **12:**544-557.
27. **Limon-Flores AY, Perez-Tapia M, Estrada-Garcia I, Vaughan G, Escobar-Gutierrez A, Calderon-Amador J, Herrera-Rodriguez SE, Brizuela-Garcia A, Heras-Chavarria M, Flores-Langarica A, Cedillo-Barron L, Flores-Romo L.** 2005. Dengue virus inoculation to human skin explants: an effective approach to assess in situ the early infection and the effects on cutaneous dendritic cells. Int J Exp Pathol **86:**323-334.
28. **Lanciotti RS, Kosoy OL, Laven JJ, Velez JO, Lambert AJ, Johnson AJ, Stanfield SM, Duffy MR.** 2008. Genetic and serologic properties of Zika virus associated with an epidemic, Yap State, Micronesia, 2007. Emerging infectious diseases **14:**1232-1239.
29. **Perera-Lecoin M, Meertens L, Carnec X, Amara A.** 2014. Flavivirus entry receptors: an update. Viruses **6:**69-88.
30. **Honda K, Yanai H, Negishi H, Asagiri M, Sato M, Mizutani T, Shimada N, Ohba Y, Takaoka A, Yoshida N, Taniguchi T.** 2005. IRF-7 is the master regulator of type-I interferon-dependent immune responses. Nature **434:**772-777.

31. **Dick GW, Kitchen SF, Haddow AJ.** 1952. Zika virus. I. Isolations and serological specificity. Transactions of the Royal Society of Tropical Medicine and Hygiene **46:**509-520.
32. **Lim PY, Behr MJ, Chadwick CM, Shi PY, Bernard KA.** 2011. Keratinocytes are cell targets of West Nile virus in vivo. J Virol **85:**5197-5201.
33. **Cerny D, Haniffa M, Shin A, Bigliardi P, Tan BK, Lee B, Poidinger M, Tan EY, Ginhoux F, Fink K.** 2014. Selective susceptibility of human skin antigen presenting cells to productive dengue virus infection. PLoS Pathog **10:**e1004548.
34. **Chen Y, Maguire T, Hileman RE, Fromm JR, Esko JD, Linhardt RJ, Marks RM.** 1997. Dengue virus infectivity depends on envelope protein binding to target cell heparan sulfate. Nat Med **3:**866-871.
35. **Germi R, Crance JM, Garin D, Guimet J, Lortat-Jacob H, Ruigrok RW, Zarski JP, Drouet E.** 2002. Heparan sulfate-mediated binding of infectious dengue virus type 2 and yellow fever virus. Virology **292:**162-168.
36. **Hilgard P, Stockert R.** 2000. Heparan sulfate proteoglycans initiate dengue virus infection of hepatocytes. Hepatology **32:**1069-1077.
37. **Kroschewski H, Allison SL, Heinz FX, Mandl CW.** 2003. Role of heparan sulfate for attachment and entry of tick-borne encephalitis virus. Virology **308:**92-100.
38. **Lee E, Pavy M, Young N, Freeman C, Lobigs M.** 2006. Antiviral effect of the heparan sulfate mimetic, PI-88, against dengue and encephalitic flaviviruses. Antiviral Res **69:**31-38.
39. **Navarro-Sanchez E, Altmeyer R, Amara A, Schwartz O, Fieschi F, Virelizier JL, Arenzana-Seisdedos F, Despres P.** 2003. Dendritic-cell-specific ICAM3-grabbing non-integrin is essential for the productive infection of human dendritic cells by mosquito-cell-derived dengue viruses. EMBO Rep **4:**723-728.
40. **Tassaneetrithep B, Burgess TH, Granelli-Piperno A, Trumpfheller C, Finke J, Sun W, Eller MA, Pattanapanyasat K, Sarasombath S, Birx DL, Steinman RM, Schlesinger S, Marovich MA.** 2003. DC-SIGN (CD209) mediates dengue virus infection of human dendritic cells. J Exp Med **197:**823-829.
41. **Chen ST, Lin YL, Huang MT, Wu MF, Cheng SC, Lei HY, Lee CK, Chiou TW, Wong CH, Hsieh SL.** 2008. CLEC5A is critical for dengue-virus-induced lethal disease. Nature **453:**672-676.
42. **Lemke G, Rothlin CV.** 2008. Immunobiology of the TAM receptors. Nat Rev Immunol **8:**327-336.
43. **Fredericksen BL, Keller BC, Fornek J, Katze MG, Gale M.** 2008. Establishment and maintenance of the innate antiviral response to West Nile Virus involves both RIG-I and MDA5 signaling through IPS-1. J Virol **82:**609-616.
44. **Bustos-Arriaga J, Garcia-Machorro J, Leon-Juarez M, Garcia-Cordero J, Santos-Argumedo L, Flores-Romo L, Mendez-Cruz AR, Juarez-Delgado FJ, Cedillo-Barron L.** 2011. Activation of the innate immune response against DENV in normal non-transformed human fibroblasts. PLoS Negl Trop Dis **5:**e1420.
45. **Nazmi A, Dutta K, Hazra B, Basu A.** 2014. Role of pattern recognition receptors in flavivirus infections. Virus Res **185:**32-40.
46. **Paladino P, Cummings DT, Noyce RS, Mossman KL.** 2006. The IFN-independent response to virus particle entry provides a first line of antiviral defense that is independent of TLRs and retinoic acid-inducible gene I. J Immunol **177:**8008-8016.
47. **Proost P, Vynckier AK, Mahieu F, Put W, Grillet B, Struyf S, Wuyts A, Opdenakker G, Van Damme J.** 2003. Microbial Toll-like receptor ligands differentially regulate CXCL10/IP-10 expression in fibroblasts and mononuclear leukocytes in synergy with IFN-gamma and provide a mechanism for enhanced synovial chemokine levels in septic arthritis. Eur J Immunol **33:**3146-3153.
48. **Bourne N, Scholle F, Silva MC, Rossi SL, Dewsbury N, Judy B, De Aguiar JB, Leon MA, Estes DM, Fayzulin R, Mason PW.** 2007. Early production of type I interferon during West Nile

virus infection: role for lymphoid tissues in IRF3-independent interferon production. J Virol **81:**9100-9108.

49. **Xie Z, Klionsky DJ.** 2007. Autophagosome formation: core machinery and adaptations. Nat Cell Biol **9:**1102-1109.
50. **Shelly S, Lukinova N, Bambina S, Berman A, Cherry S.** 2009. Autophagy is an essential component of Drosophila immunity against vesicular stomatitis virus. Immunity **30:**588-598.
51. **Lee HK, Lund JM, Ramanathan B, Mizushima N, Iwasaki A.** 2007. Autophagy-dependent viral recognition by plasmacytoid dendritic cells. Science **315:**1398-1401.
52. **Tallóczy Z, Virgin HW, Levine B.** 2006. PKR-dependent autophagic degradation of herpes simplex virus type 1. Autophagy **2:**24-29.
53. **Lee YR, Lei HY, Liu MT, Wang JR, Chen SH, Jiang-Shieh YF, Lin YS, Yeh TM, Liu CC, Liu HS.** 2008. Autophagic machinery activated by dengue virus enhances virus replication. Virology **374:**240-248.
54. **Heaton NS, Randall G.** 2011. Dengue virus and autophagy. Viruses **3:**1332-1341.
55. **Krejbich-Trotot P, Gay B, Li-Pat-Yuen G, Hoarau JJ, Jaffar-Bandjee MC, Briant L, Gasque P, Denizot M.** 2011. Chikungunya triggers an autophagic process which promotes viral replication. Virol J **8:**432.
56. **Li JK, Liang JJ, Liao CL, Lin YL.** 2012. Autophagy is involved in the early step of Japanese encephalitis virus infection. Microbes Infect **14:**159-168.
57. **Vandergaast R, Fredericksen BL.** 2012. West Nile virus (WNV) replication is independent of autophagy in mammalian cells. PLoS One **7:**e45800.
58. **Panyasrivanit M, Greenwood MP, Murphy D, Isidoro C, Auewarakul P, Smith DR.** 2011. Induced autophagy reduces virus output in dengue infected monocytic cells. Virology **418:**74-84.
59. **Ke PY, Chen SS.** 2011. Activation of the unfolded protein response and autophagy after hepatitis C virus infection suppresses innate antiviral immunity in vitro. J Clin Invest **121:**37-56.
60. **Dreux M, Gastaminza P, Wieland SF, Chisari FV.** 2009. The autophagy machinery is required to initiate hepatitis C virus replication. Proc Natl Acad Sci U S A **106:**14046-14051.
61. **Heaton NS, Randall G.** 2010. Dengue virus-induced autophagy regulates lipid metabolism. Cell Host Microbe **8:**422-432.
62. **Grard G, Caron M, Mombo IM, Nkoghe D, Mboui Ondo S, Jiolle D, Fontenille D, Paupy C, Leroy EM.** 2014. Zika virus in Gabon (Central Africa)--2007: a new threat from Aedes albopictus? PLoS Negl Trop Dis **8:**e2681.
63. **Benedict MQ, Levine RS, Hawley WA, Lounibos LP.** 2007. Spread of the tiger: global risk of invasion by the mosquito Aedes albopictus. Vector Borne Zoonotic Dis **7:**76-85.
64. **Medlock JM, Hansford KM, Schaffner F, Versteirt V, Hendrickx G, Zeller H, Van Bortel W.** 2012. A review of the invasive mosquitoes in Europe: ecology, public health risks, and control options. Vector Borne Zoonotic Dis **12:**435-447.

856

857 **FIGURE LEGENDS**

858 **Figure 1: Primary human fibroblasts are susceptible to ZIKV**. (A) Primary fibroblasts
859 infected with ZIKV (MOI1) and mock-infected cells were analyzed at different times post-
860 infection for the presence of the viral envelope protein by immunofluoresence with the 4G2
861 mAb and an FITC-conjugated anti-mouse IgG. (B) Viral replication was determined by
862 plaque assay analysis of culture supernatants of ZIKV-infected cells. (C) Expression of viral
863 RNA was determined by real-time RT-PCR. Data are representative of three independent
864 experiments each performed in duplicate (error bars represent standard error of the mean).
865 Wilcox–Mann–Whitney test was employed to analyze the difference between sets of data.
866 *indicates p values < 0.05.

867

868 **Figure 2: ZIKV infects human keratinocytes and induces morphological changes in**
869 **human skin biopsies**
870 (A) Primary human keratinocytes or (B) human skin biopsies were infected with ZIKV (MOI
871 1 and 10^6 PFU, respectively) and expression of viral RNA was determined at different time
872 points by real-time RT-PCR. Data are representative of three independent experiments each
873 performed in duplicate (error bars represent standard error of the mean). Wilcox–Mann–
874 Whitney test was employed to analyze the difference between sets of data. *indicates p values
875 < 0.05. Microscopic observation of (C) Mock- or (D and E) ZIKV-infected human skin
876 biopsies. Small arrows indicate keratinocyte cytoplasmic vacuolation. Large arrow indicates a
877 superficial sub-corneous edema with also cytoplasmic vacuolation. Magnification 20x. Data
878 are representative of two independent experiments.

879

880

Figure 3: Dendritic cells are permissive to ZIKV and DENV.

Human immature dendritic cells were infected with ZIKV or DENV (MOI 1) for 24 hpi and the intracellular presence of the viral envelope protein was detected using the pan-flavivirus Ab 4G2 by flow cytometry. Mean fluorescence intensity was determined and the percentage of infected cells was calculated, as compared to non-infected cells. Data are representative of three independent experiments.

Figure 4: Entry receptors involved in ZIKV infection

(A) Expression profile of different cell surface receptors by HEK293T cells stably expressing DC-SIGN, TIM-1, TIM-4, AXL or Tyro3 (white histograms) or parental, non-transfected cells (grey histograms). (B) HEK293T cells expressing the indicated receptors were incubated with ZIKV (MOI 0.1 and 1) and the percentage of infected cells was determined by measuring the expression of viral envelope protein by flow cytometry at 24 hpi. Data are representative of three independent experiments.

Figure 5: Involvement of AXL and TIM-1 in ZIKV infection of A549 cells

(A) Cell surface expression levels of AXL, TIM-1 and DC-SIGN on A549 cells, as determined by flow cytometry. Immunofluorescence staining of cells with specific mAb (white histogram) is superimposed on those with isotype control mAb (grey histograms). (B) A549 cells were incubated with ZIKV (MOI 1) for 1 hr at 4°C in the presence of neutralizing anti-TIM-1 (5µg/mL) and/or anti-AXL (10µg/mL), respectively, or with different concentration of a goat IgG as control. The percentage of infected cells was measured by flow cytometry and normalized to that in presence of control IgG. Data are shown as representative flow cytometry analysis (upper panel) and are represented as mean +/-SEM of at least three independent experiments (lower panel). (C) A549 cells were transfected by the indicated

siRNA, and TIM-1 and AXL expression was assessed by flow cytometry after 24hpi, at the time of infection. (D) Cells were infected with ZIKV (MOI 1). Infection was normalized to infection in nontargeting (siNT) siRNA-transfected cells. To test the significance of the differences, analysis of the variance (ANOVA) was performed with GraphPad Prism software. Statistically significant differences between each condition and control cells are denoted by an asterisk (*) and are indicated p values < 0.05. Data are representative of three independent experiments.

Figure 6: Expression of AXL permits ZIKV infection of skin fibroblasts

(A) Cell surface expression levels of AXL and TIM-1 on HFF1 cells was monitored by flow cytometry. Immunofluorescence staining of cells with specific mAb (white histogram) is superimposed on those with isotype control mAb (grey histograms). (B) HFF1 cells were incubated with ZIKV (MOI 3) or DENV (MOI 5) for 1 hr at 4°C in the presence of neutralizing anti-AXL, or normal goat IgG as control. The percentage of infected cells was measured by flow cytometry and normalized to that in presence of control IgG. Data are shown as representative flow cytometry analysis (upper panel) and are represented as mean +/-SEM of at least three independent experiments (lower panel). (C) HFF1 cells were transfected by the indicated siRNA for 24h then cells were infected with ZIKV (MOI 3) or DENV (MOI 5). Infection was normalized to infection in non-targeting (siNT) siRNA-transfected cells. To test the significance of the differences, analysis of the variance (ANOVA) was performed with GraphPad Prism software. Statistically significant differences between each condition and control cells are denoted by an asterisk (*) and are indicated p values < 0.05. Data are representative of three independent experiments.

Figure 7: ZIKV induces an innate anti-viral response in primary human skin fibroblasts

(A) Primary human fibroblasts were exposed to ZIKV (MOI 1) and mRNA levels were quantified over time by real-time RT-PCR. Results are expressed as fold induction of transcripts in ZIKV-infected cells relative to those in mock-infected cells. Data are representative of three independent experiments each performed in duplicate (errors bars represent standard error of the mean). Wilcoxon–Mann–Whitney test was employed to analyze the difference between sets of data. A value of $p < 0.05$ was considered significant. * indicates p values < 0.05. (B) Cells were exposed to ZIKV (MOI 1) at the indicated time and MX1 protein levels were detected by Western blotting using a specific antibody. The immunoblot was stripped and reblotted with an anti-α-tubulin Ab as a control for protein loading. Data are representative of three independent experiments.

Figure 8: Effect of PRR silencing on ZIKV replication and IFN expression

(A-D) siRNAs specific for MDA5 (siRNA-MDA5), RIG-I (siRNA-RIG-I), TLR3 (siRNA-TLR3), TLR7 (siRNA-TLR7), as well as a non-specific siRNA (siRNA-Ctrl), were transfected into HFF1 cells 24 h before infection with ZIKV (MOI 0.1). Reduction of mRNA levels by siRNA was confirmed by real-time RT-PCR at 24 and 48 hpi. Results are expressed as fold induction of expression of transcripts in specific siRNA-transfected cells, relative to that in siRNA-Ctrl-transfected cells. The latter value corresponds to 1 on the ordinate of each histogram. Data are representative of two independent experiments, each performed in triplicate, and are normalized according to 18S mRNA levels in the samples (errors bars represent standard error of the mean). The Wilcoxon–Mann–Whitney test was used to analyze the difference between sets of data. A value of $p < 0.05$ was considered significant and denoted by an asterisk (*). (E) Viral copy numbers in siRNA-transfected cells were measured by real-time RT-PCR at 24 and 48 hpi. Statistically significant differences (p values < 0.05) between specific siRNA- and siRNA-Ctrl-transfected cells were determined using the analysis

of the variance (ANOVA) with GraphPad Prism software and denoted by an asterisk (*). Data are representative of two independent experiments each performed in triplicate.

Figure 9: IFNs inhibit ZIKV infection

Primary skin fibroblasts were pretreated 6 h before infection with different concentrations IFN-α, IFN-β and IFN-γ and were then exposed to ZIKV at MOI 1. (A-C) inhibition of viral replication was measured, at 24 hpi, by real-time RT-PCR and (D-F) the release of viral particle quantified by plaque assay in the culture supernatants. Statistical significance of the data, were determined using analysis of the variance (ANOVA) and GraphPad Prism software and are denoted by an asterisk (*) and p values < 0.05. Data are representative of three independent experiments each performed in duplicate (error bars represent standard error of the mean).

Figure 10: Electron microscopic imaging of ZIKV-infected primary fibroblasts. (A) Membrane vesicles with size between 70 and 100 nm observed in intimate association with endoplasmic reticulum are indicated by white arrow. Black arrows indicate the presence of spherical capsids detected in intracellular vacuoles or docked to intracellular membranes. (B) Enlargement of a ZIKV particle. Intracellular electron dense spherical capsid is 40 nm in size. (C) Assembled capsids are transported to the cell surface in intracellular vacuoles. (D) Autophagosomes are frequently detected in infected fibroblasts and assembled capsids are observed inside this compartment. Data are representative of two independent experiments.

Figure 11: ZIKV induces autophagy in infected skin fibroblasts. (A) Visualization of autophagosome formation by LC3 aggregation in Mock- or ZIKV-infected cells and cells treated with Torin 1. Cells were fixed 24 hpi and the colocalization of autophagosomes and

ZIKV was determined by immunofluorescence using mAbs specific for LC3 or the viral envelope protein (4G2). Data are representative of three independent experiments. (B) Primary human skin fibroblasts were exposed to ZIKV (MOI 2) in the absence (cells were treated with the vehicle 0.05% DMSO) or presence of (B) Torin 1 or (C) 3-MA, at the indicated concentrations, and viral replication was quantified by real-time RT-PCR at 24 and 48 hpi. Data are representative of three independent experiments. To test the significance of the differences, analysis of the variance (ANOVA) was performed with GraphPad Prism software. Statistically significant differences between each condition and control cells are denoted by an asterisk (*) and are indicated by p values < 0.05.

992 **TABLES**

993 **Table 1:** Modulation of antiviral gene expression by ZIKV infection

	ZIKV[a]			ZIKV			ZIKV	
Time post-infection	6h	24h		6h	24h		6h	24h
Gene			Gene			Gene		
AIM2	**5,77**	**19,67**	IFIH1	-1,37	**7,30**	MEFV	**-648,97**	**2,62**
APOBEC3G	**3,31**	**2,64**	IFNA1	**2,34**	**3,36**	MX1	1,08	**27,44**
ATG5	-1,14	1,06	IFNA2	-1,71	-1,36	MYD88	-1,03	1,76
AZI2	1,24	1,96	IFNAR1	-1,35	-1,30	NFKB1	1,22	1,63
CARD8	-1,71	-1,36	IFNB1	-1,71	**3,70**	NFKBIA	**-3,32**	1,55
CASP1	**2,82**	**2,67**	IKBKB	1,67	1,06	NLRP3	-1,71	1,12
CASP10	**3,27**	**3,31**	IL12A	1,53	-1,10	NOD2	-1,71	-1,36
CASP8	1,96	1,31	IL12B	-1,73	-1,36	OAS2	1,14	**16,66**
CCL3	-1,71	-1,36	IL15	-1,04	1,27	PIN1	1,62	1,09
CCL5	1,52	**5,65**	IL18	-1,63	-1,74	PSTPIP1	-1,19	1,05
CD40	1,90	-1,14	IL1B	**-3,21**	**-5,29**	PYCARD	1,79	1,80
CD80	-1,71	-1,36	IL6	1,13	**8,21**	PYDC1	-1,36	-1,36
CD86	-1,71	**152,01**	IL8	**-2,83**	**3,73**	RELA	1,16	-1,05
CHUK	1,01	-1,16	IRAK1	1,40	1,61	RIPK1	1,62	1,40
CTSB	1,11	-1,00	IRF3	-1,14	-1,08	SPP1	-1,88	-1,27
CTSL1	-1,00	-1,11	IRF5	**-2,03**	1,26	STAT1	1,07	1,75
CTSS	**2,48**	**2,07**	IRF7	1,25	**3,16**	SUGT1	1,28	-1,00
CXCL10	**-47,90**	**12,54**	ISG15	-1,10	**8,33**	TBK1	-1,20	1,07
CXCL11	**-6,24**	**2,05**	JUN	**5,73**	**2,53**	TICAM1	1,49	1,52
CXCL9	**-5,55**	-1,36	MAP2K1	-1,02	-1,12	TLR3	**2,08**	**2,73**
CYLD	-1,92	-1,55	MAP2K3	-1,02	1,01	TLR7	-1,71	-1,36

DAK	**2,00**	**2,28**	MAP3K1	**2,34**	-1,48	TLR8	-1,71	-1,36
DDX3X	1,27	-1,06	MAP3K7	-1,15	-1,29	TLR9	-1,00	**-2,25**
DDX58	**-3,16**	**4,88**	MAPK1	1,26	1,01	TNF	-1,71	**-2,13**
DHX58	1,76	**2,64**	MAPK14	1,37	-1,22	TRADD	1,50	1,26
FADD	-1,34	-1,08	MAPK3	1,42	1,25	TRAF3	-1,59	1,35
FOS	-1,93	**2,29**	MAPK8	-1,21	-1,26	TRAF6	1,32	-1,13
HSP90AA1	1,42	1,44	MAVS	-1,02	-1,53	TRIM25	1,43	1,83

[a]Values represent fold-inductions of mRNA copy numbers in infected cells relative to mock-infected condition.

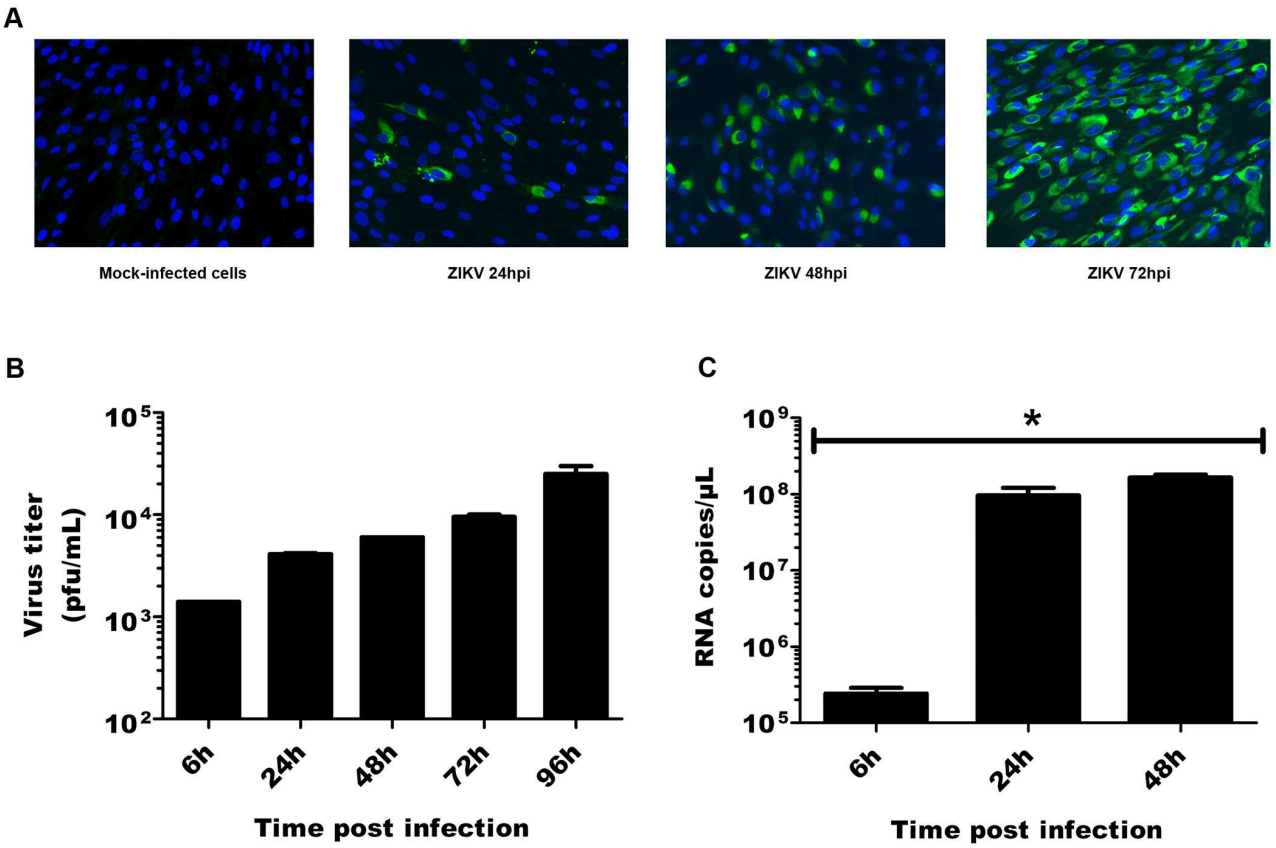

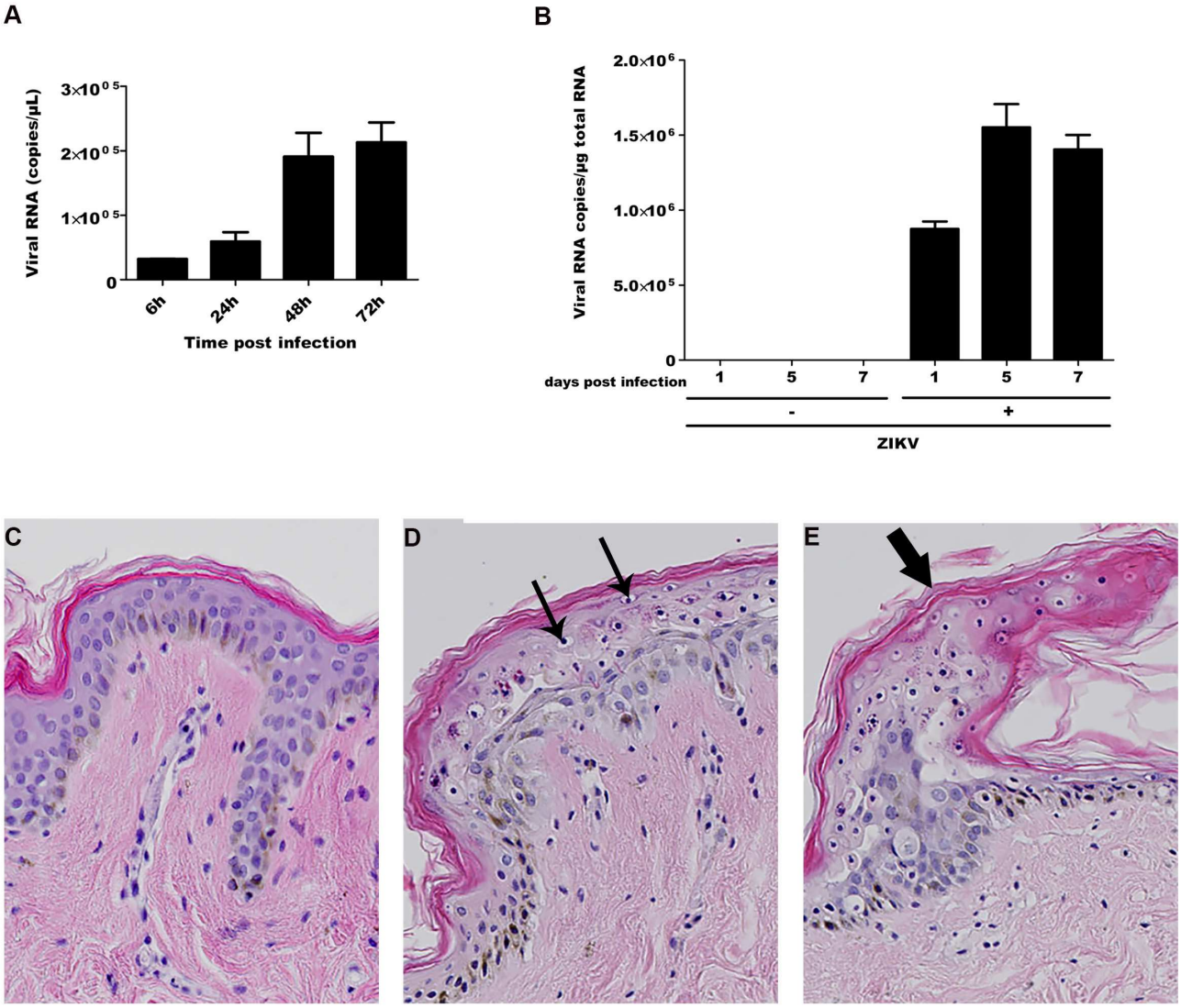

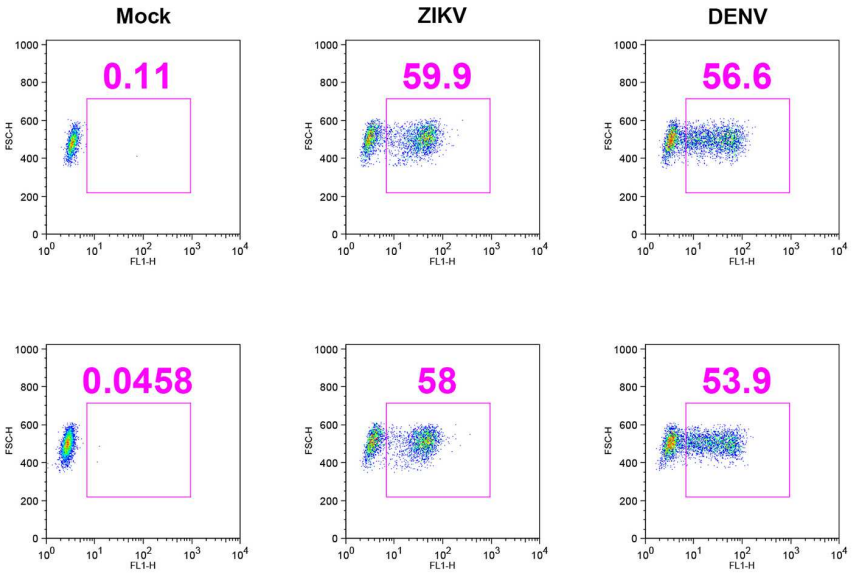

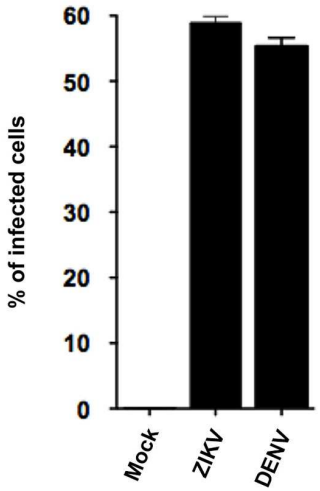

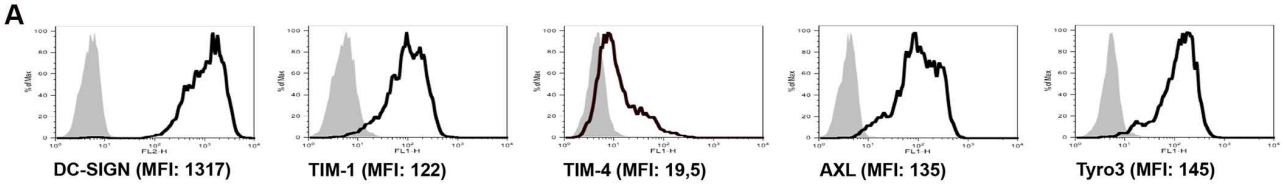

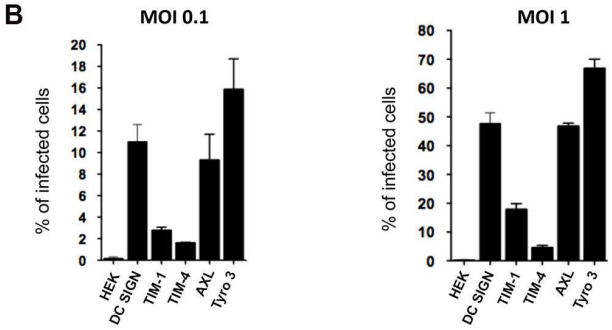

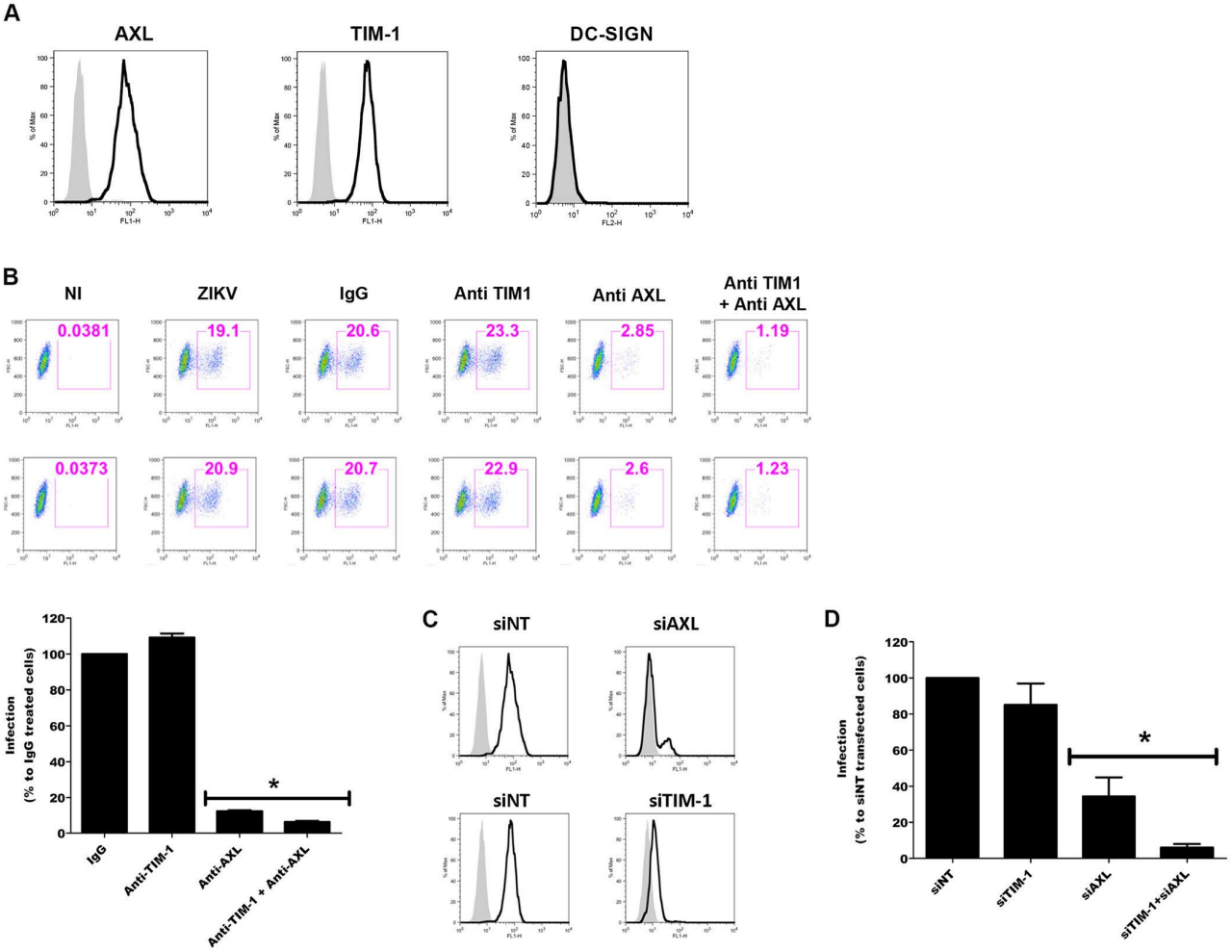

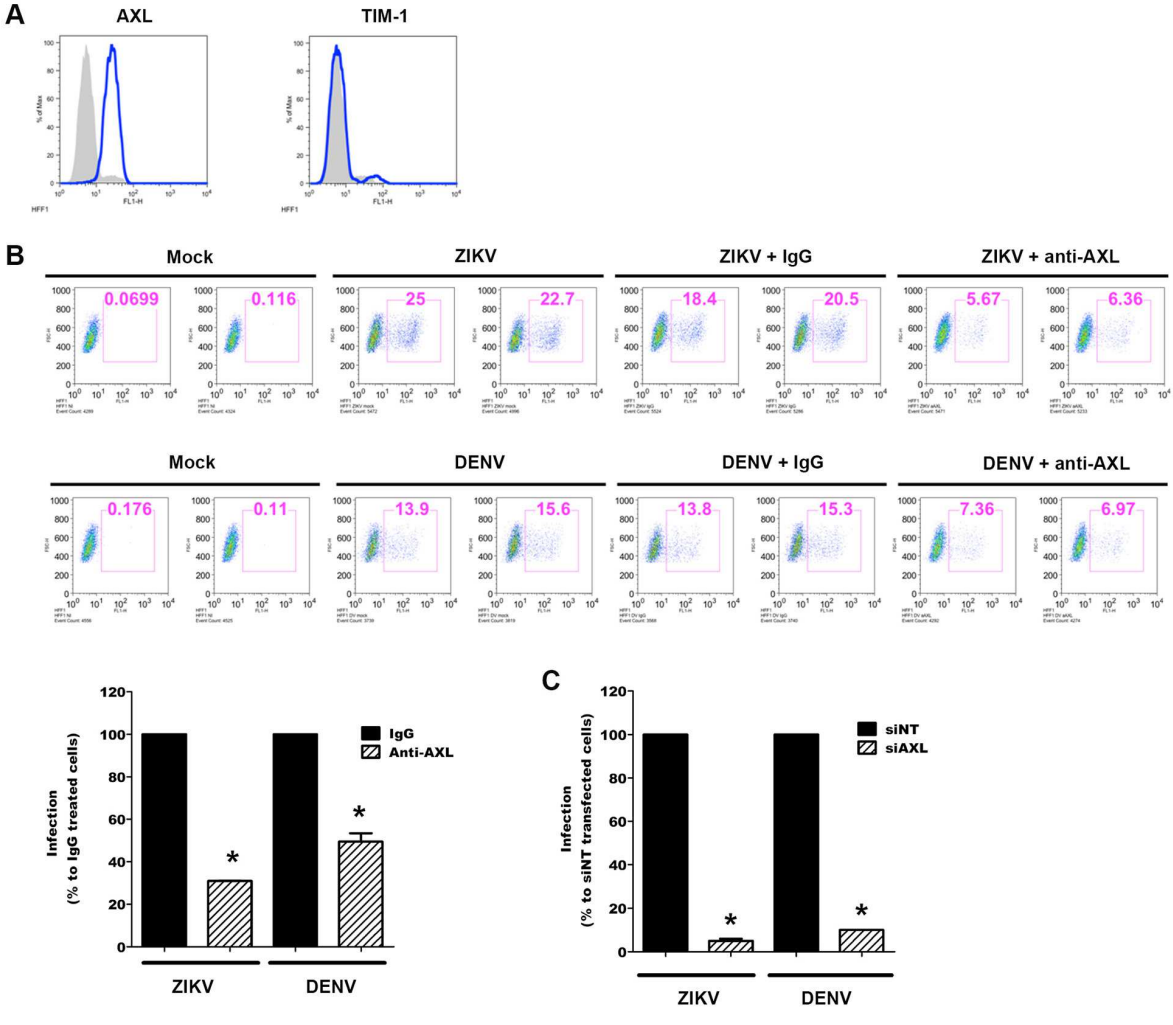

Journal of Virology